

# Towards Data-Driven Autonomics in Data Centers

Alina Sîrbu, Ozalp Babaoglu

Department of Computer Science and Engineering, University of Bologna

Mura Anteo Zamboni 7, 40126 Bologna, Italy

Email: [alina.sirbu@unibo.it](mailto:alina.sirbu@unibo.it), [ozalp.babaoglu@unibo.it](mailto:ozalp.babaoglu@unibo.it)

**Abstract**—Continued reliance on human operators for managing data centers is a major impediment for them from ever reaching extreme dimensions. Large computer systems in general, and data centers in particular, will ultimately be managed using predictive computational and executable models obtained through data-science tools, and at that point, the intervention of humans will be limited to setting high-level goals and policies rather than performing low-level operations. *Data-driven autonomics*, where management and control are based on holistic predictive models that are built and updated using generated data, opens one possible path towards limiting the role of operators in data centers. In this paper, we present a data-science study of a public Google dataset collected in a 12K-node cluster with the goal of building and evaluating a predictive model for node failures. We use BigQuery, the big data SQL platform from the Google Cloud suite, to process massive amounts of data and generate a rich feature set characterizing machine state over time. We describe how an ensemble classifier can be built out of many Random Forest classifiers each trained on these features, to predict if machines will fail in a future 24-hour window. Our evaluation reveals that if we limit false positive rates to 5%, we can achieve true positive rates between 27% and 88% with precision varying between 50% and 72%. We discuss the practicality of including our predictive model as the central component of a data-driven autonomic manager and operating it on-line with live data streams (rather than off-line on data logs). All of the scripts used for BigQuery and classification analyses are publicly available from the authors’ website.

**Keywords**-Data science; predictive analytics; Google cluster trace; log data analysis; failure prediction; machine learning classification; ensemble classifier; random forest; BigQuery

## I. INTRODUCTION

Modern data centers are the engines of the Internet that run e-commerce sites, cloud-based services accessed from mobile devices and power the social networks utilized each day by hundreds of millions of users. Given the pervasiveness of these services in many aspects of our daily lives, continued availability of data centers is critical. And when continued availability is not possible, service degradations and outages need to be foreseen in a timely manner so as to minimize their impact on users. For the most part, current automated data center management tools are limited to low-level infrastructure provisioning, resource allocation, scheduling or monitoring tasks with no predictive capabilities. This leaves the brunt of the problem in detecting and resolving undesired behaviors to armies of operators who

continuously monitor streams of data being displayed on monitors. Even at the highly optimistic rate of 26,000 servers managed per staffer<sup>1</sup>, this situation is not sustainable if data centers are ever to reach exascale dimensions. Applying traditional autonomic computing techniques to large data centers is problematic since their complex system characteristics prohibit building a “cause-effect” system model that is essential for closing the control loop. Furthermore, current autonomic computing technologies are reactive and try to steer the system back to desired states only after undesirable states are actually entered — they lack predictive capabilities to anticipate undesirable states in advance so that proactive actions can be taken to avoid them in the first place.

If data centers are the engines of the Internet, then data is their fuel and exhaust. Data centers generate and store vast amounts of data in the form of logs corresponding to various events and errors in the course of their operation. When these computing infrastructure logs are augmented with numerous other internal and external data channels including power supply, cooling, management actions such as software updates, server additions/removal, configuration parameter changes, network topology modifications, or operator actions to modify electrical wiring or change the physical locations of racks/server/storage devices, data centers become ripe to benefit from data science. The grand challenge is to exploit the toolset of modern data science and develop a new generation of autonomics that is *data-driven*, *predictive* and *proactive* based on holistic models that capture a data centre as an *ecosystem* including not only the computer system as such, but also its physical as well as its socio-political environment.

In this paper we present the results of an initial study towards building predictive models for node failures in data centers. The study is based on a recent Google dataset containing workload and scheduler events emitted by the Borg cluster management system [1] in a cluster of over 12,000 nodes during a one-month period [2], [3]. We employed BigQuery [4], a big data tool from the Google Cloud Platform that allows running SQL-like queries on massive data, to perform an exploratory feature analysis. This step generated a large number of features at various levels of

<sup>1</sup>Delfina Eberly, Director of Data Center Operations at Facebook, speaking on “Operations at Scale” at the *7x24 Exchange 2013 Fall Conference*.

aggregation suitable for use in a machine learning classifier. The use of BigQuery has allowed us to complete the analysis for large amounts of data (table sizes up to 12TB containing over 100 billion rows) in reasonable amounts of time.

For the classification study, we employed an ensemble that combines the output of multiple *Random Forests* (RF) classifiers, which themselves are ensembles of Decision Trees. RF were employed due to their proven suitability in situations where the number of features is large [5] and the classes are “unbalanced” [6] such that one of the classes consists mainly of “rare events” that occur with very low frequency. Although individual RF were better than other classifiers that were considered in our initial tests, they still exhibited limited performance, which prompted us to pursue an *ensemble approach*. While individual trees in RF are based on subsets of features, we used a combination of *bagging* and data *subsampling* to build the RF ensemble and tailor the methodology to this particular dataset. Our ensemble classifier was tested on several days from the trace data, resulting in very good performance on some days (up to 88% true positive rate, TPR, and 5% false positive rate, FPR), and modest performance on other days (minimum of 27% TPR at the same 5% FPR). Precision levels in all cases remained between 50% and 72%. We should note that these results are comparable to other failure prediction studies in the field.

The contributions of our work are severalfold. First, we advocate that modern data centers can be scaled to extreme dimensions only by eliminating reliance on human operators by adopting a new generation of autonomies that is data-driven and based on holistic predictive models. Towards this goal, we provide a failure prediction analysis for a dataset that has been studied extensively in the literature from other perspectives. The model we develop has very promising predictive power and has the potential to form the basis of a data-driven autonomic manager for data centers. Secondly, we propose an ensemble classification methodology tailored to this particular problem where subsampling is combined with bagging and precision-weighted voting to maximize performance. Thirdly, we provide one of the first examples of BigQuery usage in the literature with quantitative evaluation of running times as a function of data size. All of the scripts used for BigQuery and classification analysis are publicly available from our website [7] under the GNU General Public License.

The rest of this paper is organized as follows. The next section describes the process of building features from the trace data. Section III describes our classification approach while our prediction results are presented in Section IV. Related work is discussed in Section V. In Section VI we discuss the issues surrounding the construction of a data-driven autonomic controller based on our predictive model and argue its practicality. Section VII concludes the paper.

## II. BUILDING THE FEATURE SET WITH BIGQUERY

The workload trace published by Google contains several tables monitoring the status of the machines, jobs and tasks during a period of approximately 29 days for a cluster of 12,453 machines. This includes task events (over 100 million records, 17GB uncompressed), which follow the state evolution for each task, and task usage logs (over 1 billion records, 178GB uncompressed), which report the amount of resources per task at approximately 5 minute intervals. We have used the data to compute the overall load and status of different cluster nodes at 5 minute intervals. This resulted in a time series for each machine and feature that spans the entire trace (periods when the machine was “up”). We then proceeded to obtain several features by aggregating measures in the original data. Due to the size of the dataset, this aggregation analysis was performed using BigQuery on the trace data directly from Google Cloud Storage. We used the *bq* command line tool for the entire analysis, and our scripts are available online through our Web site [7].

From task events, we obtained several time series for each machine with a time resolution of 5 minutes. A total of 7 features were extracted, which count the number of tasks currently *running*, the number of tasks that have *started* in the last 5 minutes and those that have *finished* with different exit statuses — *evicted*, *failed*, *finished normally*, *killed* or *lost*. From task usage data, we obtained 5 additional features (again at 5-minute intervals) measuring the load at machine level in terms of: *CPU*, *memory*, *disk time*, *cycles per instruction* (CPI) and *memory accesses per instruction* (MAI). This resulted in a total of 12 *basic features* that were extracted. For each feature, at each time step we consider the previous 6 time windows (corresponding to the machine status during the last 30 minutes) obtaining 72 features in total (12 basic features  $\times$  6 time windows).

The procedure for obtaining the basic features was extremely fast on the BigQuery platform. For task counts, we started with constructing a table of running tasks, where each row corresponds to one task and includes its start time, end time, end status and the machine it was running on. Starting from this table, we could obtain the time series for each feature for each machine, requiring between 139 and 939 seconds on BigQuery per feature (one separate table per feature was obtained). The features related to machine load were computed by summing over all tasks running on a machine in each time window, requiring between 3585 and 9096 seconds on BigQuery per feature. The increased execution time is due to the increased table sizes (over 1 billion rows). We then performed a JOIN of all above tables to combine the basic features into a single table with 104,197,215 rows (occupying 7GB). For this analysis, our experience allows us to judge BigQuery as being extremely fast; an equivalent computation would have taken months to

Aggregation	Average, SD, CV	Correlation
1h	166 (all features)	45(6.5)
12h	864 (all features)	258.8(89.1)
24h	284.6(86.6)	395.6(78.9)
48h	593.6(399.2)	987.2(590)
72h	726.6(411.5)	1055.47(265.23)
96h	739.4(319.4)	1489.2(805.9)

Table I: Running times required by BigQuery for obtaining features aggregated over different time windows, for two aggregation types: computing *averages*, *standard deviation* (SD) and *coefficient of variation* (CV) versus computing *correlations*. For 1h and 12h windows, average, SD and CV were computed for all features in a single query. For all other cases, the mean (and standard deviation) of the required times per feature are shown.

perform on a regular PC.

A second level of aggregation meant looking at features over longer time windows rather than just the last 5 minutes. At each time step, 3 different statistics — averages, standard deviations and coefficients of variation — were computed for each basic feature obtained at the previous step. This was motivated by the suspicion that not only feature values but also their deviation from the mean could be important in understanding system behavior. Six different running windows of sizes 1, 12, 24, 48, 72 and 96 hours were used to capture behavior at various time resolutions. This resulted in 216 additional features (3 statistics  $\times$  12 features  $\times$  6 window sizes).

In order to generate these aggregated features, a set of intermediate tables were used. For each time point, these tables consisted of the entire set of data points to be averaged. For instance, for 1-hour averages, the table would contain a set of 6 values for each feature and for each time point, showing the evolution of the system over the past hour. While generating these tables was not time consuming (requiring between 197 and 960 seconds), their sizes were quite impressive: ranging from 143 GB (over 1 billion rows) for 1 hour up to 12.5 TB (over 100 billion rows) in the case of 96-hour window. Processing these tables to obtain the aggregated features of interest required significant resources and would not have been possible without the BigQuery platform. Even then, direct queries using a single GROUP BY operation to obtain all 216 features was not possible, requiring only one basic feature to be handled at a time and combining the results into a single table at the end. Table I shows statistics over the time required to obtain one feature for the different window sizes.

Although independent feature values are important, another criterion that could be important for prediction is the relations that exist between different measures. Correlation between features is one such measure, with different correlation values indicating changes in system behavior. Hence we introduced a third level of aggregation of the

data by computing correlations between a chosen set of feature pairs, again over various window sizes (1 to 96 hours as before). We chose 7 features to analyze: number of running, started and failed jobs together with CPU, memory, disk time and CPI. By computing correlations between all possible pairings of the 7 features, we obtained a total of 21 correlation values for each window size. This introduces 126 additional features to our dataset. The BigQuery analysis started from the same intermediate tables as before and computed correlations for one feature pair at a time. As can be seen in Table I, this step was more time consuming, requiring greater time than the previous aggregation step, yet still remains manageable considering the size of the data. The amount of data processed for these queries ranged from 49.6GB (per feature pair for 1-hour windows) to 4.33TB (per feature pair for 96-hour windows), resulting in a higher processing cost (5 USD per TB processed). Yet again, a similar analysis would not have been possible without the BigQuery platform.

The Google trace also reports machine events. These are scheduler events corresponding to machines being added or removed from the pool of resources. Of particular interest are REMOVE events, which can be due to two causes: machine failures or machine software updates. The goal of this work is to predict REMOVE events due to *machine failures*, so the two causes have to be distinguished. Prompted by our discussions, publishers of the Google trace investigated the best way to perform this distinction and suggested to look at the length of time that machines remain down — the time from the REMOVE event of interest to the next ADD event for the same machine. If this “down time” is large, then we can assume that the REMOVE event was due to a machine failure, while if it is small, the machine was most likely removed to perform a software update. To ensure that an event considered to be a failure is indeed a real failure, we used a relatively-long “down time” threshold of 2 hours, which is greater than the time required for a typical software update. Based on this threshold, out of a total of 8,957 REMOVE events, 2,298 were considered failures, and were the target of our predictive study. For the rest of the events, for which we cannot be sure of the cause, the data points in the preceding 24-hour window were removed completely from the dataset. An alternative would have been considering them part of the SAFE class, however this might not be true for some of the points. Thus, removing them completely ensures that all data labeled as SAFE are in fact SAFE.

To the above features based mostly on load measures, we added two new features: the *up time* for each machine (time since the last corresponding ADD event) and number of REMOVE events for the entire cluster within the last hour. This resulted in a total of 416 features for 104,197,215 data points (almost 300GB of processed data). Figure 1 displays the time series for 4 selected features (and the REMOVE events) at one typical machine.

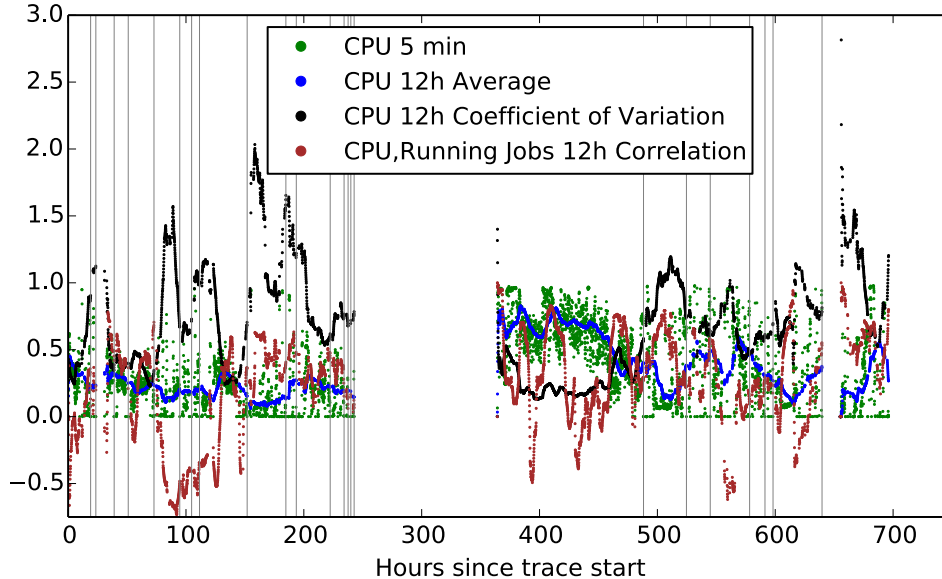


Figure 1: Four time series (4 out of 416 features) for one machine in the system. The features shown are: CPU for the last time window, CPU averages over 12 hours, CPU coefficient of variation for the last 12 hours and correlation between CPU and number of running jobs in the last 12 hours. Grey vertical lines indicate times of REMOVE events, some followed by gaps during which the machine was unavailable. The large gap from  $\sim 250$  hours to  $\sim 370$  hours is an example of a long machine downtime, following a series of multiple failures (cluster of grey vertical lines around 250 hours). In this case, the machine probably needed more extensive investigation and repair before being inserted back in the scheduler pool.

### III. CLASSIFICATION APPROACH

The features obtained in the previous section were used for classification with the *Random Forest* (RF) classifier. The data points were separated into two classes: SAFE (negatives) and FAIL (positives). To do this, for each data point (corresponding to one machine at a certain time point) we computed *time\_to\_remove* as the time to the next REMOVE event. Then, all points with *time\_to\_remove* less than 24 hours were assigned to the class FAIL while all others were assigned to the class SAFE. We extracted all the FAIL data points corresponding to real failures (108,365 data points) together with a subset of the SAFE class, corresponding to 0.5% of the total by random subsampling (544,985 points after subsampling). We used this procedure to deal with the fact that the SAFE class is much larger than the FAIL class and classifiers have difficulty learning patterns from very imbalanced datasets. Subsampling is one way of reducing the extent of this imbalance [8]. Even after this subsampling procedure, negatives are about five times the number of positives. These 653,350 data points (SAFE plus FAIL) formed the basis of our predictive study.

Given the large number of features, some might be more useful than others, hence we explored two types of feature selection mechanisms. One was *principal component analysis*, which uses the original features to build a set of principal components — additional features that account for most of the variability in the data. Then one can use

only the top principal components for classification, since those should contain the most important information. We trained classifiers with an increasing number of principal components, however the performance obtained was not better than using the original features. A second mechanism was to filter the original features based on their correlation to the time to the next failure event (*time\_to\_remove* above). Correlations were in the interval  $[-0.3, 0.45]$ , and we used only those features with absolute correlation larger than a threshold. We found that the best performance was obtained with a null threshold, which means again using all features. Hence, our attempts to reduce the feature set did not produce better results than the RF trained directly on the original features. One reason for this may be the fact that the RF itself performs feature selection when training the Decision Trees. It appears that the RF mechanism performs better in this case than correlation-based filtering or principal component analysis.

To evaluate the performance of our approach, we employed cross validation. Given the procedure we used to define the two classes, there are multiple data points corresponding to the same failure (data over 24 hours with 5 minutes resolution). Since some of these data points are very similar, choosing the *train* and *test* data cannot be done by selecting random subsets. While random selection may give extremely good prediction results, it is not realistic since we would be using test data which is too similar to the training

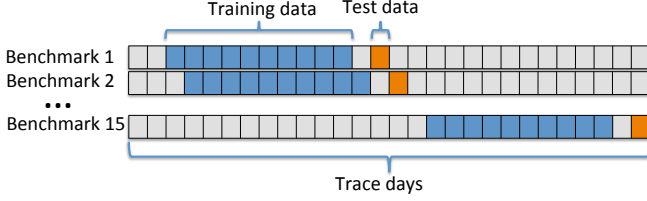


Figure 2: Cross validation approach: forward-in-time testing. Ten days were used for training and one day for testing. A set of 15 benchmarks (train/test pairs) were obtained by sliding the train/test window over the 29-day trace.

data. This is why we opted for a time-based separation of train and test data. We considered basing the training on data over a 10-day window, followed by testing based on data over the next day with no overlap with the training data. Hence, the test day started 24 hours after the last training data point. The first two days were omitted in order to decrease the effect on aggregated features. In this manner, fifteen train/test pairs were obtained and used as benchmarks to evaluate our analysis (see Figure 2). This forward-in-time cross validation procedure ensures that classification performance is realistic and not an artifact of the structure of the data. Also, it mimics the way failure prediction would be applied in a live data center, where every day a model could be trained on past data to predict future failures.

Given that many points from the FAIL class are very similar, which is not the case for the SAFE class due to initial subsampling, the information in the SAFE class is still overwhelmingly large. This prompted us to further subsample the negative class in order to obtain the training data. This was performed in such a way that the ratio between SAFE and FAIL data points is equal to a parameter  $fsafe$ . We varied this parameter with the values  $\{0.25, 0.5, 1, 2, 3, 4\}$  while using all of the data points from the positive class so as not to miss any useful information. This applied only for training data: for testing we always used all data from both the negative and positive classes (out of the base dataset of 653,350 points). We also used RF of different sizes, with the number of Decision Trees varying from 2 to 15 with a step of 1 (resulting in 14 different values).

As we will discuss in the following section, the performance of the individual classifiers, while better than random, was judged to be not satisfactory. This is why we opted for an ensemble method, which builds a series of classifiers and then selects and combines them to provide the final classification. Ensembles can enhance the power of low performing individual classifiers [5], especially if these are diverse [9], [10]: if they give false answers on different data points (independent errors), then combining their knowledge can improve accuracy. To create diverse classifiers, one can vary the model parameters but also train them with different data (known as the *bagging* method [5]). Bagging matches

very well with subsampling to overcome the rare events problem, and in fact it has been shown to be effective for the class-imbalance problem [8]. Hence, we adopt a similar approach to build our individual classifiers. Every time a new classifier is trained, a new training dataset is built by considering all the data points in the positive class and a random subset of the negative class. As described earlier, the size of this subset is defined by the  $fsafe$  parameter. By varying the value of  $fsafe$  and number of trees in the RF algorithm, we created diverse classifiers. The following algorithm details the procedure used to build the individual classifiers in the ensemble.

```

Require:  $train\_pos, train\_neg, Shuffle(), Train()$ 
 $fsafe \leftarrow \{0.25, 0.5, 1, 2, 3, 4\}$ 
 $tree\_count \leftarrow \{2..15\}$ 
 $classifiers \leftarrow \{\}$ 
 $start \leftarrow 0$ 
for all  $fs \in fsafe$  do
  for all  $tc \in tree\_count$  do
     $end \leftarrow start + fs * |train\_pos|$ 
    if  $end \geq |train\_neg|$  then
       $start \leftarrow 0$ 
       $end \leftarrow start + fs * |train\_pos|$ 
       $Shuffle(train\_neg)$ 
    end if
     $train\_data \leftarrow train\_pos + train\_neg[start: end]$ 
     $classifier \leftarrow Train(train\_data, tc)$ 
     $append(classifiers, classifier)$ 
     $start \leftarrow end$ 
  end for
end for

```

We repeated this procedure 5 times, resulting in 5 classifiers for each combination of the parameters  $fsafe$  and RF size. This resulted in a total of 420 RF in the ensemble (5 repetitions  $\times$  6  $fsafe$  values  $\times$  14 RF sizes).

Once the pool of classifiers is obtained, a combining strategy has to be used. Most existing approaches use the majority vote rule — each classifier votes on the class and the majority class becomes the final decision [5]. Alternatively, a weighted vote can be used, and we opted for *precision-weighted voting*. For most existing methods, weights correspond to the accuracy of each classifier on training data [11]. In our case, performance on training data is close to perfect and accuracy is generally high, which is why we use precision on a subset of the test data. Specifically, we divide the test data into two halves: an *individual test* data set and an *ensemble test* data set. The former is used to evaluate the precision of individual classifiers and obtain a weight for their vote. The latter provides the final evaluation of the ensemble. All data corresponding to the test day was used, with no subsampling. Table II shows the number of data points used for each benchmark for training and testing. While the parameter  $fsafe$  controlled the ratio SAFE/FAIL during training, FAIL instances were much less frequent during testing, varying

Benchmark	Train			Individual Test		Ensemble Test	
	FAIL	FAIL	SAFE	FAIL	SAFE	FAIL	SAFE
1	41485	2055	9609	2055	9610		
2	41005	2010	9408	2011	9408		
3	41592	1638	9606	1638	9606		
4	42347	1770	9597	1770	9598		
5	42958	1909	9589	1909	9589		
6	42862	1999	9913	2000	9914		
7	41984	1787	9821	1787	9822		
8	39953	1520	10424	1520	10424		
9	37719	1665	10007	1666	10008		
10	36818	1582	9462	1583	9463		
11	35431	1999	9302	1999	9302		
12	35978	3786	10409	3787	10410		
13	35862	2114	9575	2114	9575		
14	39426	1449	9609	1450	9610		
15	40377	1284	9783	1285	9784		

Table II: Size of training and testing datasets. For training data, the number of SAFE data points is the number of FAIL multiplied by the *fsafe* parameter at each run.

between 13% and 36% of the number of SAFE instances.

To perform precision-weighted voting, we first applied each RF  $i$  obtained above to the *individual test data* and computed their precision  $p_i$  as the fraction of points labeled FAIL that were actually failures. In other words, *precision* is the probability that an instance labeled as a failure is actually a real failure, which is why we decided to use this as a weight. Then we applied each RF to the *ensemble test data*. For each data point  $j$  in this set, each RF provided a classification  $o_i^j$  (either 0 or 1 corresponding to SAFE or FAIL, respectively). The classification of the ensemble (the whole set of RF) was then computed as a *continuous score*

$$s_j = \sum_i o_i^j p_i \quad (1)$$

by summing individual answers weighted by their precision. Finally, these were normalized by the highest score in the data

$$s'_j = \frac{s_j}{\max_j(s_j)} \quad (2)$$

The resulting score  $s'_j$  is proportional to the likelihood that a data point is in the FAIL class — the higher the score, the more certain we are that we have an actual failure. The following algorithm outlines the procedure of obtaining the final ensemble classification scores.

**Require:** *classifiers*, *individual\_test*, *ensemble\_test*

**Require:** *Precision()*, *Classify()*

*classification\_scores*  $\leftarrow \{\}$

*weights*  $\leftarrow \{\}$

**for all**  $c \in \text{classifiers}$  **do**

$w \leftarrow \text{Precision}(c, \text{individual\_test})$

*weights*[ $c$ ]  $\leftarrow w$

**end for**

**for all**  $d \in \text{ensemble\_test}$  **do**

*score*  $\leftarrow 0$

**for all**  $c \in \text{classifiers}$  **do**

$\text{score} \leftarrow \text{score} + \text{weights}[c] * \text{Classify}(c, d)$

**end for**

*append(classification\_scores, score)*

**end for**

*max*  $\leftarrow \text{Max}(classification\_scores)$

**for all**  $s \in \text{classification\_scores}$  **do**

$s \leftarrow \text{smax}$

**end for**

It assumes that the set of classifiers is available (*classifiers*), together with the two test data sets (*individual\_test* and *ensemble\_test*) and procedures to compute precision of a classifier on a dataset (*Precision()*) and to apply a classifier to a data point (*Classify()* which returns 0 for SAFE and 1 for FAIL).

#### IV. CLASSIFICATION RESULTS

The ensemble classifier was applied to all 15 benchmark datasets. Training was done on an iMac with 3.06GHz Intel Core 2 Duo processor and 8GB of 1067MHz DDR3 memory running OSX 10.9.3. Training of the entire ensemble took between 7 and 9 hours for each benchmark dataset.

Given that the result of the classification is a continuous score (Equation 2), and not a discrete label, evaluation was based on the *Receiver Operating Characteristic* (ROC) and *Precision-Recall* (PR) curves. A class can be obtained for a data point  $j$  from the score  $s'_j$  by using a threshold  $s^*$ . A data point is considered to be in the FAIL class if  $s'_j \geq s^*$ . The smaller  $s^*$ , the more instances are classified as failures. Thus, by decreasing  $s^*$  the number of true positives grows but so do the false positives. Similarly, at different threshold values, a certain precision is obtained. The ROC curve plots the True Positive Rate (TPR) versus the False Positive Rate (FPR) of the classifier as the threshold is varied. Similarly, The PR curve displays the *precision* versus *recall* (equal to TPR or Sensitivity). It is common to evaluate a classifier by computing the *area under ROC* (AUROC) and *area under PR* (AUPR) curves, which can range from 0 to 1.

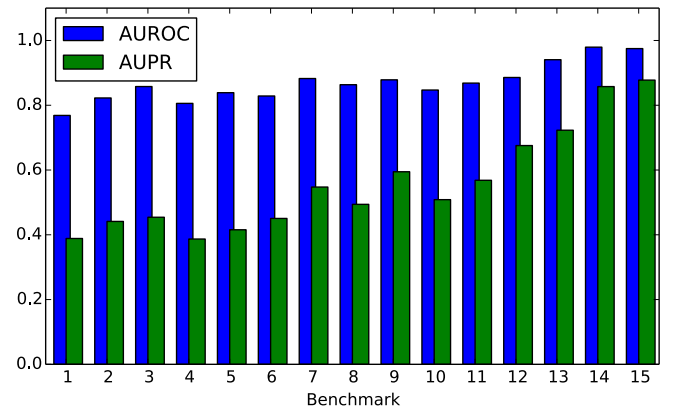


Figure 3: AUROC and AUPR on *ensemble test data* for all benchmarks.

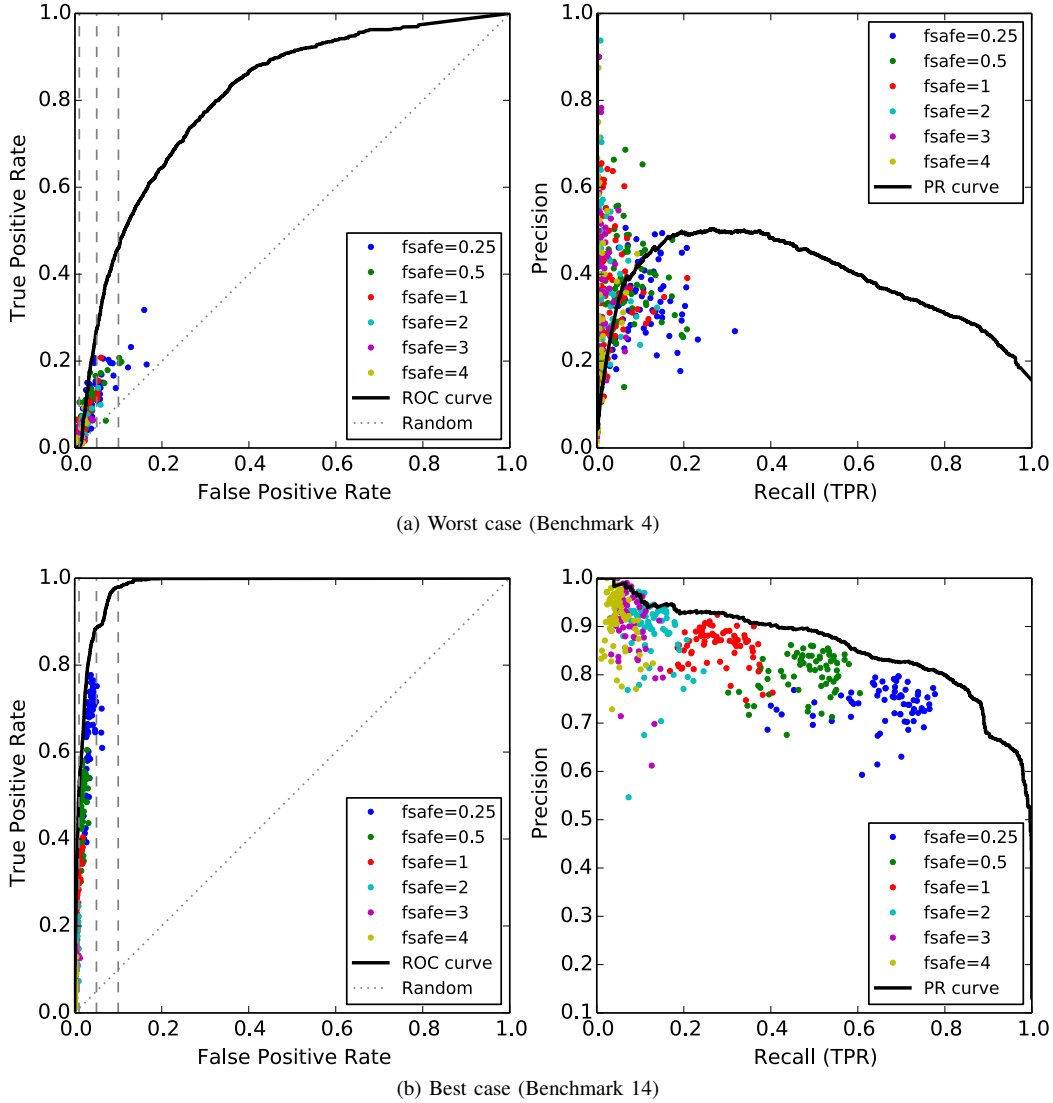


Figure 4: ROC and PR curves for worst and best performance across the 15 benchmarks (4 and 14, respectively). The vertical lines correspond to FPR of 1%, 5% and 10%. Note that parameter *fsafe* controls the ratio of SAFE to FAIL data in the training datasets.

AUROC values greater than 0.5 correspond to classifiers that perform better than random guesses, while AUPR represents an average classification precision, so, again, the higher the better. AUROC and AUPR do not depend on the relative distribution of the two classes, so they are particularly suitable for class-imbalance problems such as the one at hand.

Figure 3 shows AUROC and AUPR values obtained for all datasets, evaluated on the *ensemble test* data. For all benchmarks, AUROC values are very good, over 0.75 and up to 0.97. AUPR ranges between 0.38 and 0.87. Performance appears to increase, especially in terms of precision, towards the end of the trace. Lower performance that is observed for the first two benchmarks could be due to the fact that

some of the aggregated features (those over 3 or 4 days) are computed with incomplete data at the beginning.

To evaluate the effect of the different parameters and the ensemble approach, Figure 4 displays the ROC and PR curves for the benchmarks that result in the worst and best results (4 and 14, respectively). Performance of the individual classifiers in the ensemble are also displayed (as points in the ROC/PR space since their answer is categorical). We can see that individual classifiers result in very low FPR which is very important in predicting failures. Yet, in many cases, the TPR values are also very low. This means that most test data is classified as SAFE and very few failures are actually identified.

TPR appears to increase when the *fsafe* parameter de-

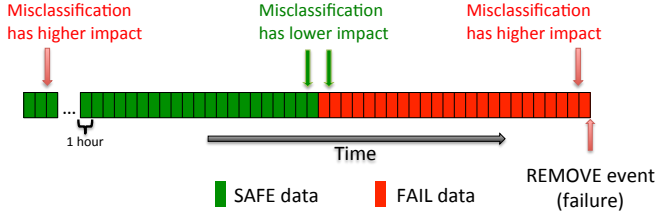


Figure 5: Representation of the time axis for one machine. The SAFE and FAIL labels are assigned to time points based on the time to the next failure. Misclassification has different impacts depending on its position on the time axis. In particular, if we misclassify a data point close to the transition from SAFE to FAIL, the impact is lower than if we misclassify far from the boundary. The latter situation would mean flagging a failure even if no failure will appear for a long time, or marking a machine as SAFE when failure is imminent.

creases, but at the expense of the FPR and Precision. The plots show quantitatively the clear dependence between the three plotted measures and  $f_{safe}$  values. As the amount of SAFE training data decreases, the classifiers become less stringent and can identify more failures, which is an important result for this class-imbalance problem. Also, the plot shows clearly that individual classifiers obtained with different values for  $f_{safe}$  are diverse, which is critical for obtaining good ensemble performance.

In general, the points corresponding to the *individual classifiers* are below the ROC and PR curves describing the performance of the *ensemble*. This proves that the ensemble method is better than the individual classifiers for this problem, which can be also due to their diversity. Some exceptions do appear (points above the solid lines), however for very low TPR (under 0.2) so in an area of the ROC/PR space that is not interesting from our point of view. We are interested in maximizing the TPR while keeping the FPR at bay. Specifically, the FPR should never grow beyond 5%, which means few false alarms. At this threshold, the two examples from Figure 4 display TPR values of 0.272 (worst case) and 0.886 (best case), corresponding to precision values of 0.502 and 0.728 respectively. This is much better than individual classifiers at this level, both in terms of precision and TPR. For failure prediction, this means that between 27.2% and 88.6% of failures are identified as such, while from all instances labeled as failures, between 50.2% and 72.8% are actual failures.

In order to analyze the implications of the obtained results in more detail, the relation between the classifier label and the exact time until the next REMOVE event was studied for the data points. This is important because we originally assigned the label SAFE to all data points that are more than 24 hours away from a failure. According to this classification, a machine would be considered to be in SAFE

state whether it fails in 2 weeks or in 2 days. Similarly, it is considered to be in FAIL state whether it fails in 23 hours or in 10 minutes. Obviously these are very different situations, and the impact of misclassification varies depending on the time to the next failure. Figure 5 displays this graphically. As the time to the next failure decreases, a SAFE data point misclassified as FAIL counts less as a misclassification, since failure is actually approaching. Similarly, a FAIL data point labeled as SAFE has a higher negative impact when it is close to the point of failure.

We would like to verify whether our classifier assigns correct and incorrect labels uniformly within each class, irrespective of the real time to the next failure. For this, Figure 6 shows the distribution of the time-to-the-next-failure, in the form of boxplots, for true positives (TP), false negatives (FN), true negatives (TN) and false positives (FP), again for the worst and best cases (benchmarks 4 and 14, respectively). We look at results obtained at 5% FPR

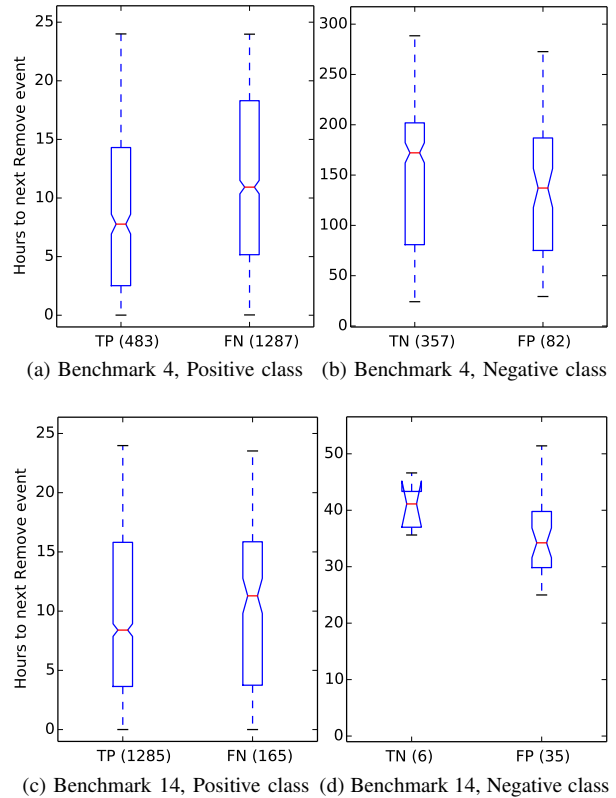


Figure 6: Distribution of time to the next machine REMOVE for data points classified, divided into True Positive (TP), False Negative (FN), True Negative (TN) and False Positive (FP). The worst and best performance (benchmarks 4 and 14, respectively) out of the 15 runs are shown. Actual numbers of instances in each class are shown in parentheses on the horizontal axis.



values. A good result would be if misclassified positives are further in time from the point of failure compared to correctly classified failures. And misclassified negatives are closer to the failure point compared to correctly classified negatives.

All positive instances, which are data points corresponding to real failures, are shown in the left panels (Figure 6a and 6c). These are divided into TP (failures correctly identified by the classifier) and FN (failures missed by the classifier). All data points have a time to the next REMOVE event between 0 and 24 hours, due to the way the positive class was defined. If the classifier was independent of the time to the next failure, the two distributions shown for TP and FN would be very similar. However, the plots show that TP have, on average, lower times until the next event, compared to FN. This means that many of the positive data points that are misclassified are further in time from the actual failure moment compared to those correctly identified. This is good news, because it suggests that although data points are not recognized as imminent failure situations when there is still some time left before the actual failure, correct classification may occur as the failure moment approaches. In fact, if we compute the fraction of failure events that are flagged at least once in the preceding 24 hour window, we obtain values larger than the TPR computed at the data-point level, especially when prediction power is lowest (52.5% vs. 27.2% for benchmark 4 and 88.7% vs. 88.6% for benchmark 14).

Negative (SAFE) instances — data points that do not precede a REMOVE event by less than 24 hours — can be divided into two classes: those for which there is a REMOVE due to a real failure before the end of the trace and those for which there is none. For the latter, we have no means to estimate the time to the next failure event. So Figures 6b and 6d show the time to the next REMOVE only for the former, i.e., those machines which will fail before the end of the trace. This is only a small fraction of the entire SAFE test data, especially for the benchmark with best performance, because it is only three days before the trace ends. However it still provides some indication on the time to the next failure of the negative class, divided into FP (negatives that are labeled as failures) and TN (negatives correctly labeled SAFE). As the figure shows, on average, times to the next failure are lower for FP compared to TN. This is again a good result because it means that many times the classifier gives false alarms when a failure is approaching, even if it is not strictly in the next 24 hours.

## V. RELATED WORK

The publication of the Google trace data has triggered a flurry of activity within the community including several with goals that are related to ours. Some of these provide general characterization and statistics about the workload and node state for the cluster [12], [13], [14] and identify

high levels of heterogeneity and dynamism in the system, especially when compared to grid workloads [15]. User profiles [16] and task usage shapes [17] have also been characterized for this cluster. Other studies have applied clustering techniques for workload characterization, either in terms of jobs and resources [18], [19] or placement constraints [20], with the aim to synthesize new traces. A different type of usage is for validation of various workload management algorithms. Examples are [21] where the trace is used to evaluate consolidation strategies, [22], [23] where over-committing (overbooking) is validated, [24] who take heterogeneity into account to perform provisioning or [25] investigating checkpointing algorithms.

System modeling and prediction studies using the Google trace data are far fewer than those performing characterization or validation. An early attempt at system modeling based on this trace [26] validates an event-based simulator using workload parameters extracted from the data, with good performance in simulating job status and overall system load. Host load prediction using a Bayesian classifier was analyzed in [27]. Using CPU and RAM history, the mean load in a future time window is predicted, by dividing possible load levels into 50 discrete states. Here we perform prediction of machine failures for this cluster, which has not been attempted to date, to our knowledge.

Failure prediction has been an active topic for many years, with a comprehensive review presented in [28]. This work summarizes several methods of failure prediction in single machines, clusters, application servers, file systems, hard drives, email servers and clients, etc., dividing them into failure tracking, symptom monitoring or error reporting. The method introduced here falls into the symptom monitoring category, however elements of failure tracking and error reporting are also present through features like number of recent failures and job failure events.

More recent studies concentrate on larger scale distributed systems such as HPC or clouds. For failure tracking methods, an important resource is the failure trace archive [29], a repository for failure logs and an associated toolkit that can enable integrated characterization of failures, such as distributions of inter-event times. Job failure in a cloud setting has been analyzed in [30]. The naive Bayes classifier is used to obtain a probability of failure based on the job type and host name. This is applied on traces from Amazon EC2 running several scientific applications. The method reaches different performances on jobs from three different application settings, with FNs of 4%, 12% and 16% of total data points and corresponding FPs of 0%, 4% and 10% of total data points. This corresponds approximately to FPR of 0%, 5.7% and 16.3%, and TPR of 86.6%, 61.2% and 58.9%. The performance we obtained with our method is within a similar range for most benchmarks, although we never reach their best performance. However, we are predicting machine and not job failures.

A comparison of different classification tools for failure prediction in an IBM Blue Gene/L cluster is given in [31]. In this work, they analyze Reliability, Availability and Serviceability (RAS) events using SVMs, neural networks, rule based classifiers and a custom nearest neighbor algorithm, trying to predict whether different event categories will appear. The custom nearest neighbor algorithm outperforms the others reaching 50% precision and 80% TPR. A similar analysis was also performed for a Blue Gene/Q cluster [32]. The best performance was again by the nearest neighbor classifier (10% FPR, 20% TPR). They never evaluated the Random Forest or ensemble algorithms.

In [33] an anomaly detection algorithm for cloud computing was introduced. It employs Principal Component Analysis and selects the most relevant principal components for each failure type. They find that higher order components are better correlated with errors. Using threshold on these principal components, they identify data points outside the normal range. They study four types of failures: CPU-related, memory-related, disk-related and network-related faults, in a controlled in-house system with fault injection and obtain very high performance, 91.4% TPR at 3.7% FPR. On a production trace (the same Google trace we are using) they predict task failures at 81.5% TPR and 27% FPR (at 5% FPR, TPR is down to about 40%). In our case, we studied the same trace but looking at machine failures as opposed to task failures, and obtained TRP values between 27% and 88% at 5% FPR.

All above-mentioned failure prediction studies concentrate on types of failures or systems different from ours and obtain variable results. In all cases, our predictions compare well with prior studies, with our best result being better than most.

## VI. DISCUSSION

Here we consider the possibility of including our predictive model in a data-driven autonomic controller for use in data centers. In such a scenario, both model building and model updating would happen on-line on data that is being streamed from various sources. From a technical point of view, on-line use would require a few changes to our model workflow.

To build the model, all features have to be computed on-line. Log data can be collected in a BigQuery table using the streaming API. As data is being streamed, features have to be computed at 5 minute intervals. Both basic and aggregated features (averages, standard deviations, coefficients of variation and correlations) have to be computed, but only for the last time window (previous time windows are already stored in a dedicated table). Basic features are straightforward to compute requiring negligible running time since they can be computed using accumulators as the events come in. For aggregated features, parallelization can be employed, since they are all independent. In our experiments, correlation

computation was most time consuming, with an average time to compute one correlation feature over the longest time window taking 1489.2 seconds for all values over the 29 days (Table I). For computing a single value (for the newly streamed data), the time required should be on average under 0.2 seconds. This estimate corresponds to a linear dependence between the number of time windows and computation time and offers an upper bound for the time required. If this stage is performed in parallel on BigQuery, this would also be the average time to compute all 126 correlation features (each feature can be computed independently so speedup would be linear).

In terms of dollar costs, we expect figures similar to those during our tests — about 60 USD per day for storage and analysis. To this, the streaming costs would have to be added — currently 1 cent per 200MB. For our system, the original raw data is about 200GB for all 29 days, so this would translate to approximately 7GB of data streamed every day for a system of similar size, leading to a cost of about 35 cents per day. At all times, only the last 12 days of features need to be stored, which keeps data size relatively low. In our analysis, for all 29 days, the final feature table requires 295GB of BigQuery storage, so 12 days would amount to about 122GB of data.

When a new model has to be trained (e.g., once a day), all necessary features are already computed. One can use an infrastructure like the Google Compute Engine to train the model, which would eliminate the need to download the data and would allow for training of the individual classifiers of the ensemble in parallel. In our tests, the entire ensemble took under 9 hours to train, with each RF requiring at most 3 minutes. Again, since each classifier is independent, training all classifiers in parallel would take under 3 minutes as well (provided one can use as many CPUs as there are RFs — 420 in our study). Combining the classifiers takes a negligible amount of time.

All in all, we expect the entire process of updating the model to take under 5 minutes if full parallelization is used both for feature computation and training. Application of the model on new data requires a negligible amount of time once features are available. This makes the method very practical for on-line use. Here we have described a cloud computing scenario, however, given the relatively limited computation and storage resources that are required, we believe that more modest clusters can also be used for monitoring, model updating and prediction.

## VII. CONCLUSIONS

We have presented a predictive study for failure of nodes in a Google cluster based on a published workload trace. Feature extraction from raw data was performed using BigQuery, the big data cloud platform from Google which enables SQL-like queries. A large number of features were generated and an ensemble classifier was trained on log data

for 10 days and tested on the following non-overlapping day. The length of the trace allowed repeating this process 15 times producing 15 benchmark datasets, with the last day in each dataset being used for testing.

The BigQuery platform was extremely useful for obtaining the features from log data. Although limits were found for JOIN and GROUP BY statements, these were circumvented by creating intermediate tables, which sometimes contained over 12TB of data. Even so, features were obtained with reduced running times, with overall cost for the entire analysis processing one month worth of logs, coming in at under 2000 USD<sup>2</sup>, resulting in a daily cost of just over 60 USD.

Classification performance varied from one benchmark to another, with Area-Under-the-ROC curve measure varying between 0.76 and 0.97 while Area-Under-the-Precision-Recall curve measure varying between 0.38 and 0.87. This corresponded to true positive rates in the range 27%-88% and precision between 50% and 72% at a false positive rate of 5%. In other words, this means that in the worst case, we were able to identify 27% of failures, while if a data point was classified as a failure, we could have 50% confidence that we were looking at a real failure. For the best case, we were able to identify almost 90% of failures and 72% of instances classified as failures corresponded to real failures. All this, at the cost of having false alarms 5% of the time.

Although not perfect, our predictions achieve good performance levels. Results could be improved by changing the subsampling procedure. Here, only a subset of the SAFE data was used due to the large number of data points in this class, and a random sample was extracted from this subset when training each classifier in the ensemble. However, one could subsample every time from the full set. However, this would require greater computational resources for training, since a single workstation cannot process 300 GB of data at a time. Training times could be reduced through parallelization, since the problem is embarrassingly parallel (each classifier in the ensemble can be trained independently from the others). These improvements will be pursued in the future. Introduction of additional features will also be explored, to take into account in a more explicit manner the interaction between machines. BigQuery will be used to obtain interactions between machines from the data, which will result in networks of nodes. Changes in the properties of these networks over time could provide important information on possible future failures.

The method presented here is very suitable for on-line use. A new model can be trained every day, using the last 12 days of logs. This is the scenario we simulated when we created the 15 test benchmarks. The model would be trained from 10 days of data and tested on one non-overlapping day, exactly like in the benchmarks (Figure 2). Then, it would

be applied for one day to predict future failures. The next day a new model would be obtained from new data. Each time, only the last 12 days of data would be used, rather than increasing the amount of training data. This to account for the fact that the system itself and the workload can change in time, so old data may not match current system behavior. This would ensure that the model is up to date with the current system state. The testing stage is required for live use for two reasons. First, part of the test data is used to build the ensemble (prediction-weighted voting). Secondly, the TPR and precision values on test data can help system administrators make decisions on the criticality of the predicted failure.

#### ACKNOWLEDGMENTS

BigQuery analysis was carried out through a generous Cloud Credits grant from Google. We are grateful to John Wilkes of Google for helpful discussions regarding the cluster trace data.

#### REFERENCES

- [1] A. Verma, L. Pedrosa, M. R. Korupolu, D. Oppenheimer, E. Tune, and J. Wilkes, "Large-scale cluster management at Google with Borg," in *Proceedings of the European Conference on Computer Systems (EuroSys)*, Bordeaux, France, 2015.
- [2] J. Wilkes, "More Google cluster data," Google research blog, Nov. 2011, Posted at <http://googleresearch.blogspot.com/2011/11/more-google-cluster-data.html>.
- [3] C. Reiss, J. Wilkes, and J. L. Hellerstein, "Obfuscatory obscanturism: making workload traces of commercially-sensitive systems safe to release," in *Network Operations and Management Symposium (NOMS), 2012 IEEE*. IEEE, 2012, pp. 1279–1286.
- [4] J. Tigani and S. Naidu, *Google BigQuery Analytics*. John Wiley & Sons, 2014.
- [5] L. Rokach, "Ensemble-based classifiers," *Artificial Intelligence Review*, vol. 33, no. 1-2, pp. 1–39, 2010.
- [6] T. M. Khoshgoftaar, M. Golawala, and J. Van Hulse, "An empirical study of learning from imbalanced data using random forest," in *Tools with Artificial Intelligence, 2007. ICTAI 2007. 19th IEEE International Conference on*, vol. 2. IEEE, 2007, pp. 310–317.
- [7] A. Sirbu and O. Babaoglu, "BigQuery and ML scripts for 'Predicting machine failures in a Google cluster'," Website, 2015, available at <http://cs.unibo.it/~sirbu/Google-trace-prediction-scripts.html>.
- [8] M. Galar, A. Fernandez, E. Barrenechea, H. Bustince, and F. Herrera, "A review on ensembles for the class imbalance problem: bagging-, boosting-, and hybrid-based approaches," *Systems, Man, and Cybernetics, Part C: Applications and Reviews, IEEE Transactions on*, vol. 42, no. 4, pp. 463–484, 2012.

<sup>2</sup>Based on current Google BigQuery pricing.

- [9] L. I. Kuncheva, C. J. Whitaker, C. A. Shipp, and R. P. Duin, "Is independence good for combining classifiers?" in *Pattern Recognition, 2000. Proceedings. 15th International Conference on*, vol. 2. IEEE, 2000, pp. 168–171.
- [10] C. A. Shipp and L. I. Kuncheva, "Relationships between combination methods and measures of diversity in combining classifiers," *Information Fusion*, vol. 3, no. 2, pp. 135 – 148, 2002.
- [11] D. W. Opitz, J. W. Shavlik *et al.*, "Generating accurate and diverse members of a neural-network ensemble," *Advances in neural information processing systems*, pp. 535–541, 1996.
- [12] C. Reiss, A. Tumanov, G. R. Ganger, R. H. Katz, and M. A. Kozuch, "Heterogeneity and Dynamicity of Clouds at Scale: Google Trace Analysis," in *ACM Symposium on Cloud Computing (SoCC)*, 2012.
- [13] —, "Towards understanding heterogeneous clouds at scale: Google trace analysis," *Carnegie Mellon University Technical Reports*, vol. ISTC-CC-TR, no. 12-101, 2012.
- [14] Z. Liu and S. Cho, "Characterizing Machines and Workloads on a Google Cluster," in *8th International Workshop on Scheduling and Resource Management for Parallel and Distributed Systems (SRMPDS)*, 2012.
- [15] S. Di, D. Kondo, and W. Cirne, "Characterization and Comparison of Google Cloud Load versus Grids," in *International Conference on Cluster Computing (IEEE CLUSTER)*, 2012, pp. 230–238.
- [16] O. A. Abdul-Rahman and K. Aida, "Towards understanding the usage behavior of Google cloud users: the mice and elephants phenomenon," in *IEEE International Conference on Cloud Computing Technology and Science (CloudCom)*, Singapore, Dec. 2014, pp. 272–277.
- [17] Q. Zhang, J. L. Hellerstein, and R. Boutaba, "Characterizing Task Usage Shapes in Google's Compute Clusters," in *Proceedings of the 5th International Workshop on Large Scale Distributed Systems and Middleware*, 2011.
- [18] A. K. Mishra, J. L. Hellerstein, W. Cirne, and C. R. Das, "Towards Characterizing Cloud Backend Workloads: Insights from Google Compute Clusters," *Sigmetrics performance evaluation review*, vol. 37, no. 4, pp. 34–41, 2010.
- [19] G. Wang, A. R. Butt, H. Monti, and K. Gupta, "Towards Synthesizing Realistic Workload Traces for Studying the Hadoop Ecosystem," in *19th IEEE Annual International Symposium on Modelling, Analysis, and Simulation of Computer and Telecommunication Systems (MASCOTS)*, 2011, pp. 400–408.
- [20] B. Sharma, V. Chudnovsky, J. L. Hellerstein, R. Rifaat, and C. R. Das, "Modeling and synthesizing task placement constraints in google compute clusters," in *Proceedings of the 2nd ACM Symposium on Cloud Computing*. ACM, 2011, p. 3.
- [21] J. O. Iglesias, L. M. Lero, M. D. Cauwer, D. Mehta, and B. O'Sullivan, "A methodology for online consolidation of tasks through more accurate resource estimations," in *IEEE/ACM Intl. Conf. on Utility and Cloud Computing (UCC)*, London, UK, Dec. 2014.
- [22] F. Caglar and A. Gokhale, "iOverbook: intelligent resource-overbooking to support soft real-time applications in the cloud," in *7th IEEE International Conference on Cloud Computing (IEEE CLOUD)*, Anchorage, AK, USA, Jun–Jul 2014. [Online]. Available: <http://www.dre.vanderbilt.edu/~gokhale/WWW/papers/CLOUD-2014.pdf>
- [23] D. Breitgand, Z. Dubitzky, A. Epstein, O. Feder, A. Glikson, I. Shapira, and G. Toffetti, "An adaptive utilization accelerator for virtualized environments," in *International Conference on Cloud Engineering (IC2E)*, Boston, MA, USA, Mar. 2014, pp. 165–174.
- [24] Q. Zhang, M. F. Zhani, R. Boutaba, and J. L. Hellerstein, "Dynamic heterogeneity-aware resource provisioning in the cloud," *IEEE Transactions on Cloud Computing (TCC)*, vol. 2, no. 1, Mar. 2014.
- [25] S. Di, Y. Robert, F. Vivien, D. Kondo, C.-L. Wang, and F. Cappello, "Optimization of cloud task processing with checkpoint-restart mechanism," in *25th International Conference on High Performance Computing, Networking, Storage and Analysis (SC)*, Denver, CO, USA, Nov. 2013.
- [26] A. Balliu, D. Olivetti, O. Babaoglu, M. Marzolla, and A. Sirbu, "Bidal: Big data analyzer for cluster traces," in *Informatika (BigSys workshop)*, vol. 232. GI-Edition Lecture Notes in Informatics, 2014, pp. 1781–1795.
- [27] S. Di, D. Kondo, and W. Cirne, "Host load prediction in a Google compute cloud with a Bayesian model," *2012 International Conference for High Performance Computing, Networking, Storage and Analysis*, pp. 1–11, Nov. 2012.
- [28] F. Salfner, M. Lenk, and M. Malek, "A survey of online failure prediction methods," *ACM Computing Surveys (CSUR)*, vol. 42, no. 3, pp. 1–68, 2010.
- [29] B. Javadi, D. Kondo, A. Iosup, and D. Epema, "The Failure Trace Archive: Enabling the comparison of failure measurements and models of distributed systems," *Journal of Parallel and Distributed Computing*, vol. 73, no. 8, 2013.
- [30] T. Samak, D. Gunter, M. Goode, E. Deelman, G. Juve, F. Silva, and K. Vahi, "Failure analysis of distributed scientific workflows executing in the cloud," in *Network and service management (cnsm), 2012 8th international conference and 2012 workshop on systems virtualization management (svm)*. IEEE, 2012, pp. 46–54.
- [31] Y. Liang, Y. Zhang, H. Xiong, and R. Sahoo, "Failure Prediction in IBM BlueGene/L Event Logs," *Seventh IEEE International Conference on Data Mining (ICDM 2007)*, pp. 583–588, Oct. 2007.
- [32] R. Dudko, A. Sharma, and J. Tedesco, "Effective Failure Prediction in Hadoop Clusters," *University of Idaho White Paper*, pp. 1–8, 2012.
- [33] Q. Guan and S. Fu, "Adaptive anomaly identification by exploring metric subspace in cloud computing infrastructures," in *32nd IEEE Symposium on Reliable Distributed Systems (SRDS)*, Braga, Portugal, Sep. 2013, pp. 205–214.